Journal of Catalysis **206,** 23–28 (2002)
doi:10.1006/jcat.2001.3463, available online at http://www.idealibrary.com on IDEAL®

Acid Properties and Catalysis of MCM-22 with Different Al Concentrations

Kazu Okumura,[1] Masashi Hashimoto, Takayuki Mimura, and Miki Niwa

Department of Materials Science, Faculty of Engineering, Tottori University, Koyama-cho Minami, Tottori 680-8552, Japan

Received April 23, 2001; revised October 30, 2001; accepted October 30, 2001; published online January 14, 2002

MCM-22 with Si/Al_2 ratios of 15–80 were hydrothermally synthesized. The acid properties and catalysis of the prepared MCM-22 were studied. The acid character changed depending on the Al concentration. Brønsted acid sites were dominant in the Si/Al_2 ratios of 42–80. These samples showed broad desorption peaks of NH_3 in the temperature-programmed desorption spectra. On the other hand, in the Si/Al_2 with ratios of 15–28, weak Lewis acid sites were dominant. The ratio of total acid against contained Al was calculated to be 32–51%. The value was characteristically lower than the stoichiometry, which suggested that only a part of Al was incorporated in the MCM-22 framework. The cracking of octane isomer and liquid-phase Friedel–Crafts acylation were carried out over MCM-22 with different amounts of Al. The catalytic performance was correlated with the structure and acid properties of MCM-22.

Key Words: **MCM-22; acid property; ^{29}Si MAS NMR; temperature-programmed desorption of ammonia; cracking; Friedel–Crafts reaction.**

INTRODUCTION

MCM-22 is a relatively new material, invented in 1990 (1). The structure of MCM-22 was first proposed by Leonowicz *et al*. based on the measurement of high-resolution micrographs and X-ray diffraction (XRD) data (2). The material has a unique structure, where two independent pore systems exist. One is the sinusoidal channel composed of circular 10-membered rings. The other is the two-dimensional supercages with 12-membered rings with 7.1-Å inner diameter and 18.2-Å inner height. MCM-22 has been tested for many kinds of reactions, such as isomerization, cracking, and chemical synthesis reactions (3–5). Unique catalytic reactions have been reported to occur due to the presence of the characteristic pore systems (6).

We have systematically measured the acid properties of many kinds of zeolites (7–13). The data obtained enabled us to compare and characterize these zeolites. The objective of this study is to measure the acid properties of MCM-22 in conjunction with structural information and catalysis.

[1] To whom correspondence should be addressed. Fax: +81-857-31-5684. E-mail: okmr@chem.tottori-u.ac.jp.

EXPERIMENTAL

Synthesis of MCM-22

MCM-22 was synthesized according to the method reported by Corma *et al*. (14). Hexamethyleneimene (nacalai tesque), Ludox HS-40 (Aldrich), and $NaAlO_2$ were used as template, Si source, and Al source, respectively. Typically, the hydrothermal synthesis was conducted at 423 K for 84 h using a Teflon-coated stainless steel autoclave, which was vertically rotated at 15 rpm. After being filtered, the as-synthesized form was calcined in air at 853 K for 3 h. The calcined sample was ion-exchanged with 0.5 M NH_4NO_3 at 353 K for 24 h, followed by calcination in a N_2 flow at 773 K to give H-form MCM-22. The chemical composition of the product was measured by an inductively coupled plasma (ICP) method after the digestion of the sample with HF solution.

MAS NMR Measurement

^{27}Al magic-angle spinning (MAS) NMR spectra were obtained on a JEOL ECP300 spectrometer with spinning speed 5.0 kHz. The ^{27}Al chemical shifts were referenced to aluminum sulfate solution (0 ppm). ^{29}Si MAS NMR spectra were obtained on a Varian INOVA-40 spectrometer with spinning speed 4.5 kHz, 5-ms excitation pulses, and 60-s recycle time. The ^{29}Si chemical shifts were referenced to polydimethylsilane (−34.1 ppm).

Temperature-Programmed Desorption of Ammonia

The acid amount was measured using temperature-programmed desorption (TPD) of ammonia. The sample was evacuated at 773 K prior to the measurement. The TPD data was collected with a ramping rate of 10 K min^{-1}. A mass spectrometer was used to monitor the desorbed NH_3. The acid amount was measured from desorbed ammonia; however, the low-temperature peak was excluded since it was not desorbed from acid sites. The water–vapor treatment to remove the *l*-peak was not conducted in this study in order to avoid experimental error due to its disturbance of acid sites (15).

0021-9517/02 $35.00

Catalytic Reactions

A conventional type of pulse reactor was used for cracking of octane isomers. A 5-mg sample was pretreated under a He stream at 773 K for 1 h. The reaction was conducted at 573 K with injection of 1 mm^3 of octane or 2,2,4-trimethylpentane in 30 $ml\,min^{-1}$ of He carrier gas flow. The cracked products were analyzed by GC equipped with a flame ionization detector (FID) and a silicone SE-30 column.

Liquid-phase Friedel–Crafts acylation was conducted under an atmosphere of nitrogen at 363 K for 2 h in a three-necked round flask. For the reaction, 46 mmol of anisole, 10 mmol of acetic anhydride, and 220 mg of catalyst were used. The products were analyzed by GC with an FID and a silicone OV-17 column, using tridecane as an internal standard.

RESULTS AND DISCUSSION

Synthesis of MCM-22

First, the influence of the rotation of the synthesis gel in the autoclave on the final zeolite structure was examined. Figure 1 shows the XRD patterns of the as-synthesized form of MCM-22 synthesized under different rotating conditions. The synthesis was carried out at 423 K while the bottle was rotated at 15 or 60 rpm for 84 h ($Si/Al_2 = 15$). As can be seen in the figure, the final structure of the product changed significantly depending on the stirring conditions. Zeolites with MCM-22 and ZSM-35 structures were obtained with rotation rates of 15 and 60 rpm, respectively. The ZSM-35 structure was also

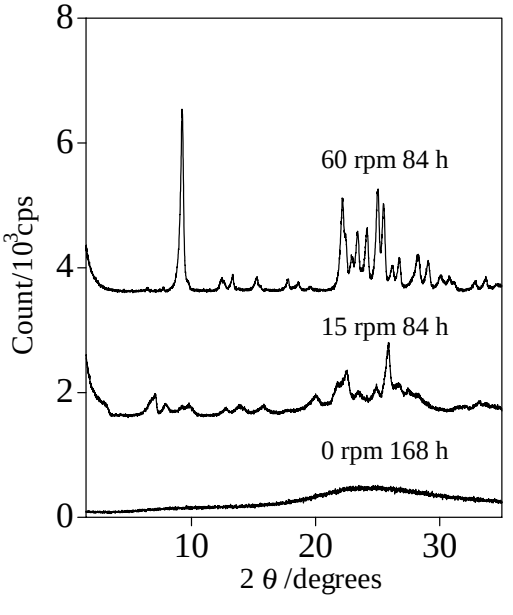

FIG. 1. XRD patterns of the form as synthesized under different stirring conditions.

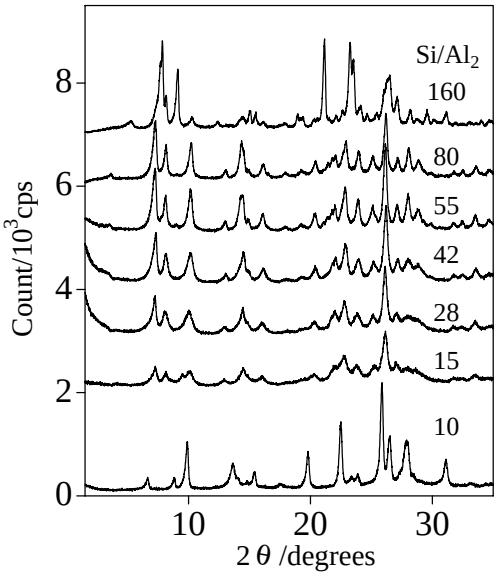

FIG. 2. XRD patterns of the H-form of the synthesized samples.

observed, even under rotation at 15 rpm, when the synthesis period exceeded 4 days. However, no zeolitic structure was found after synthesis for 7 days under static conditions. The above results indicate that the rotation of the bottle promoted the crystallization of the synthesis gel to form MCM-22 and also its successive transformation to the ZSM-35 structure. Therefore, it can be noted that the crystallization of MCM-22 is sensitive to stirring conditions as well as to the synthesis period.

In the following, the hydrothermal synthesis of MCM-22 was conducted at 15 rpm for 84 h. Figure 2 shows the XRD patterns of the H-form of zeolites synthesized by varying the Al concentration of the initial gel. MCM-22 was obtained from Si/Al_2 with ratios between 15 and 80, whereas zeolites with Si/Al_2 ratios of 10 and 160 were identified to be MOR (mordenite) and MTW (ZSM-12), respectively. Thus, it was confirmed that synthesis of the MCM-22 crystal is possible in the narrow region of Al concentration between 15 and 80. The fact agrees with the results reported by Mochida *et al.* (16). The transformation of the as-synthesized form to the H-form resulted in an increase in the sharpness of the peaks. The highest intensity was obtained on MCM-22 with $Si/Al_2 = 55$.

N_2 Adsorption Isotherms and ^{29}Si MAS NMR

The surface area and pore volume calculated based on the N_2 adsorption isotherms are listed in Table 1. MCM-22 with $Si/Al_2 = 55$ showed the highest surface area and pore volume. The tendency agreed with the XRD patterns, where the highest intensity was observed in the sample with $Si/Al_2 = 55$. The pore volume of MCM-22 was reported to be 0.20 $cm^3\,g^{-1}$, which was comparable to that observed in the present sample (17).

TABLE 1

The Surface Area and Pore Volume of MCM-22

Si/Al_2 ratio	Al concn (mol kg^{-1})	Surface area (m^2 g^{-1})	Pore volume (cm^3 g^{-1})
15	1.99	530	0.16
28	1.14	589	0.17
42	0.77	629	0.19
55	0.59	661	0.20
80	0.41	492	0.15

Figure 3a shows the ^{27}Al MAS NMR of the H-form MCM-22. The peaks situated at 53 and 0 ppm were straightforwardly assigned to the tetrahedral (Td) and octahedral (Oh) Al species. Both Td and Oh Al species were observed

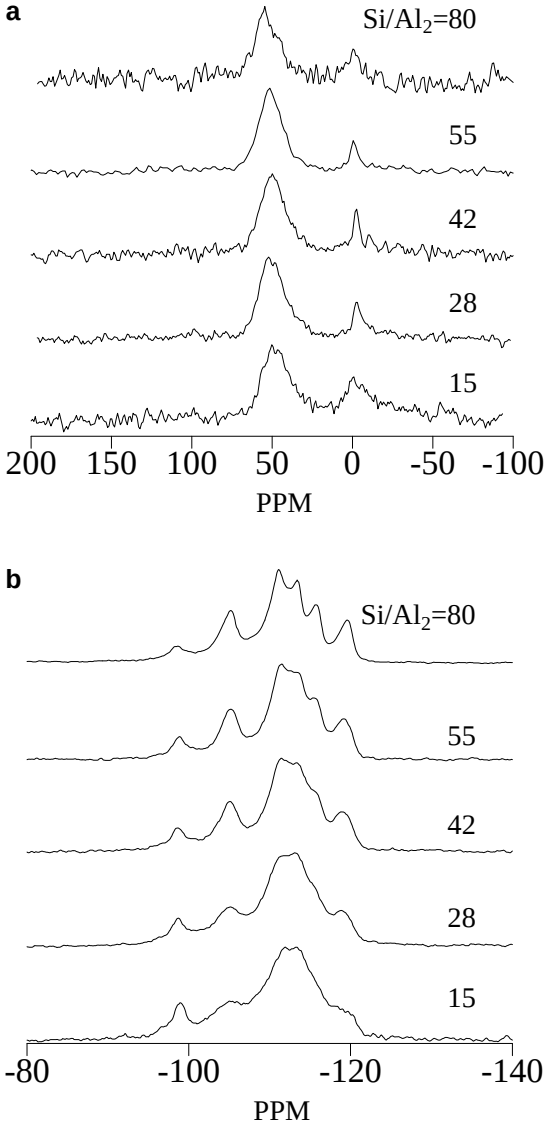

FIG. 3. (a) ^{27}Al and (b) ^{29}Si MAS NMR spectra of the H-form MCM-22.

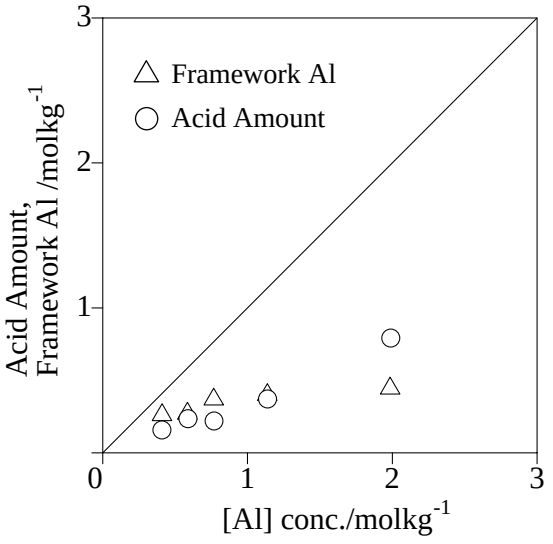

FIG. 4. Dependence of Al content on the amount of framework Al estimated by ^{29}Si NMR (△) and the amount of acid measured by NH_3 TPD (○).

in every sample. The presence of the Oh Al suggested that part of the Al was situated outside the MCM-22 framework. Figure 3b shows ^{29}Si MAS NMR of the H-form MCM-22 with different Al content. The peaks became broader with increased Al concentration. It was reported that the peaks that appeared between −120 and −110 ppm were mainly composed of Si(0Al) species. The appearance of five peaks is a consequence of the wide distribution of T–O–T bonds ranging from 138° to 164° (18). On the other hand, the peak at −98 ppm was primarily due to the Si(1Al) species (19). Indeed, the intensity of the line increased with the Al concentration of the samples. The Al incorporated into the lattice of MCM-22 was calculated based on the assumption that the peak at −98 ppm was originated from Si(1Al) and peaks between −120 and −110 ppm were due to the Si(0Al) species. The content of the framework Al was estimated by using the simplified equation (20)

$$(Si/Al)_{NMR} = \left[I_{Si(0Al)} + I_{Si(1Al)}\right]/0.25 I_{Si(1Al)}. \qquad [1]$$

$I_{Si(0Al)}$ and $I_{Si(1Al)}$ are the sum of the area between −120 and −110 ppm and the area of the peak at −98 ppm, respectively. Figure 4 gives the dependence of the Al concentration in the framework of MCM-22 on the total Al in the sample. The MCM-22 framework was estimated to be 22–64% of the total Al content. That fact meant that only part of the Al was present in the MCM-22 framework even in the samples with low Al concentrations ($Si/Al_2 =$ 42–80). The value increased with decreased Al concentration.

Acid Properties

IR of pyridine was measured in order to determine the kind of acid sites generated on MCM-22. Figure 5a shows

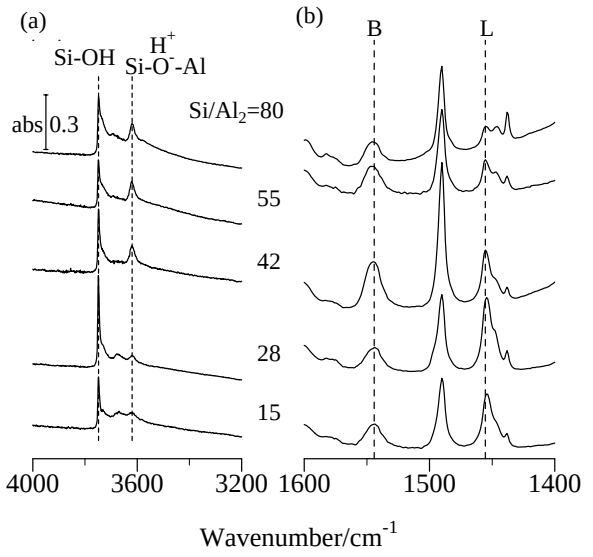

FIG. 5. Fourier transform IR spectra of (a) MCM-22 evacuated at 773 K and (b) pyridine adsorbed on MCM-41.

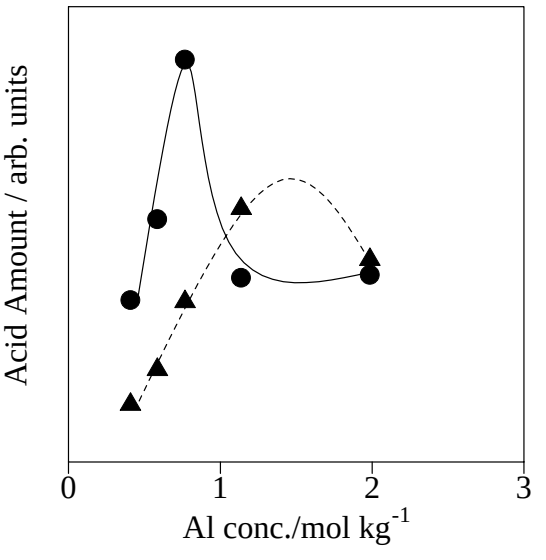

FIG. 6. Dependence of Al content on the relative acid concentration of MCM-22 measured by IR of adsorbed pyridine: ●, Brønsted acid; ▲, Lewis acid.

the IR spectra of MCM-22 measured after evacuation at 773 K. The absorption bands due to the isolated silanol groups and acid sites appeared at 3759 and 3620 cm^{-1}, respectively. The intense peak due to the acid sites could be seen in the Si/Al_2 range between 42 and 80. The peak became weaker with further increases in Al content. At the same time, a small peak appeared at 3669 cm^{-1}, which was ascribed to the extraframework Al species (21). The change in the acidic OH group indicated that the Brønsted acid sites are dominant in the MCM-22 with $Si/Al_2 = 42–80$. However, it was lower in the samples with $Si/Al_2 = 15$ and 28.

Figure 5b shows the IR of pyridine exposed to H-form MCM-22 at room temperature, followed by evacuation at 473 K. Pyridine adsorbed on Brønsted and Lewis acid sites appeared at 1544 and 1455 cm^{-1}, respectively. The relative amount of pyridine adsorbed on these two kinds of acid sites was plotted against Al concentration of MCM-22 in Fig. 6. The molar extinction coefficients of pyridine on Brønsted and Lewis sites were taken into consideration in the calculation (22). Brønsted acid sites are dominant with Si/Al_2 ratios of 42–80, whereas Lewis acid sites exceed the Brønsted acidity in the sample with Si/Al_2 ratios of 15 and 28. Therefore, it is noted that the kind of acidity generated on MCM-22 is dependent on the Al content and its distribution changes with Si/Al_2 ratios between 28 and 42. The present change in the intensity of the pyridine adsorbed on the Brønsted acid sites paralleled that of the acidic OH group observed in Fig. 5a.

Figure 7 shows NH_3 TPD of MCM-22 with different Al concentrations. The desorbed amount of NH_3 plotted against Al concentrations of MCM-22 is given in Fig. 4. In the spectra of MCM-22 with $Si/Al_2 = 42–80$, the value was calculated by subtracting the area of the *l*-peak that appeared at ca. 450 K from the total desorbed amount of NH_3, since the *l*-peak was not considered to have originated from the real acid sites (8). The acid amount corresponded to only 32–51% of the total Al content in MCM-22. Such a discrepancy has not been observed on mordenite, ZSM-5, and β-zeolite and is a significant character of this zeolite species. The discrepancy became clear with an increase in total Al content. However, the acid amount almost coincided with Al content in the framework measured from ^{29}Si NMR spectra, except for MCM-22 with $Si/Al_2 = 15$, as can be seen in Fig. 4. Therefore, the low concentrations of

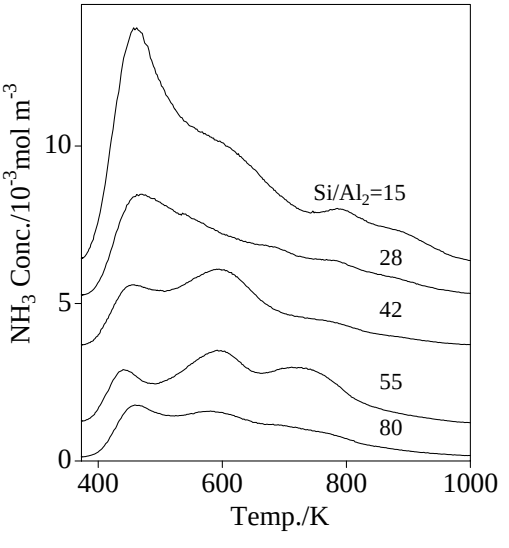

FIG. 7. NH_3 TPD of MCM-22 with different Al contents.

acid relative to that of Al are attributed to the fact that the portion of Al incorporated into the MCM-22 framework was low.

Catalytic Reactions

Cracking reactions of octane isomers were conducted over MCM-22. Figure 8 shows the dependence of the conversion of octane and 2,2,4-trimethylpentane on the Al content of MCM-22. Octane cracked over MCM-22 with the conversion of 7–23%, where the maximum value was obtained on the MCM-22 with $Si/Al_2 = 42$. The tendency agreed with the Brønsted acidity measured by IR shown in Fig. 6. In contrast, 2,2,4-trimethylpentane was totally inactive in the reaction under the same conditions. That fact means that the MCM-22 behaves similarly to the 10-membered ring zeolite for this reaction. The phenomenon agrees with the constraint index data, CI* (23). That is to say, it was reported that MCM-22 exhibited a CI* value of 4.6, which was characteristic of a 10-member ring (24). In this case, owing to the restricted ability of 2,2,4-dimethylpentane to penetrate into the MCM-22 pore composed of 10-membered rings, the occurrence of the cracking reaction was hindered.

The liquid-phase reaction between acetophenone and acetic anhydride (Friedel–Crafts acylation) was conducted over H-form MCM-22. This reaction is an important method for synthesizing aromatic ketones. *p*-Methoxyacetophenone was detected as the single product of the reaction. The material balance calculated based on the anisole (reactant) and *p*-methoxyacetophenone (product) was $100 \pm 2\%$. The yield of *p*-methoxyacetophenone was

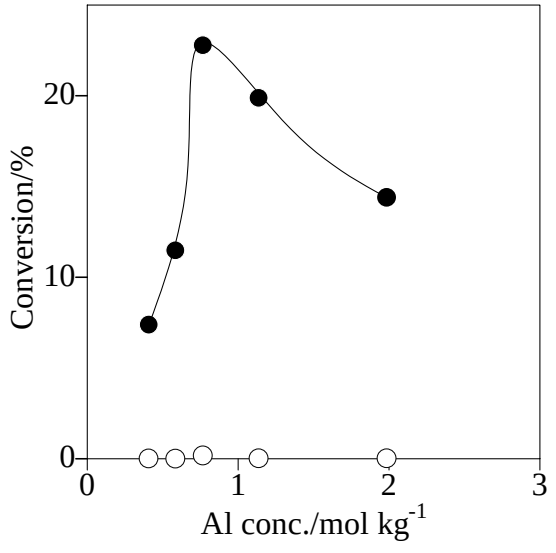

FIG. 8. The conversion of octane isomer plotted against Al content of MCM-22: ●, octane; ○, 2,2,4-trimethylpentane. The reaction was conducted using the pulse method. Temperature, 573 K.

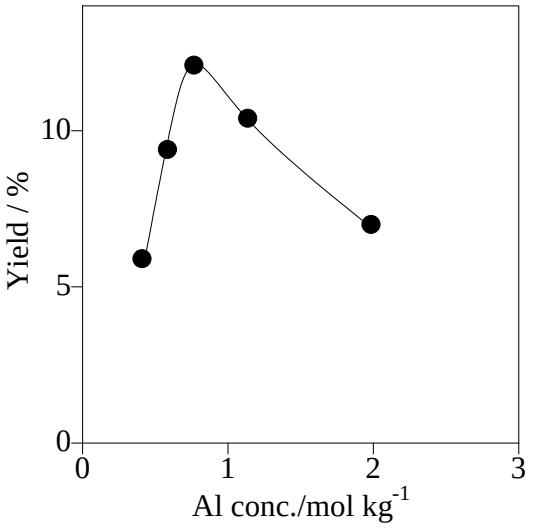

FIG. 9. Yield of *p*-methoxyacetophenone in the reaction of anisole and acetic anhydride plotted against the Al content of MCM-22: reaction temperature, 423 K; reaction time, 2 h.

plotted against the Al content of MCM-22 in Fig. 9. Again, the conversion agreed with the change in the Brønsted acid concentration measured by IR, where the maximum Brønsted acid amount was attained at $Si/Al_2 = 42$. For comparison, the reaction was conducted over β-type zeolite (PQ company, $Si/Al_2 = 20$), which was reported to be the most efficient zeolite for the reaction (25). The β-zeolite afforded *p*-methoxyacetophen-one with 29% yield. Though the maximum yield of *p*-methoxyacetophenone on MCM-22 was lower than that on β-zeolite, the yields were comparable when compared on the basis of Al content, since the Al content of the MCM-22 sample with $Si/Al_2 = 42$ was half that of the β-zeolite sample. That fact suggested that MCM-22 is a promising catalyst for application in liquid-phase Friedel–Crafts reactions.

CONCLUSIONS

Some insights into the synthesis conditions and acid properties of MCM-22 were obtained through the combination of several characterization methods. The final structure was highly dependent on the temperature and rotation during the hydrothermal synthesis. MCM-22 has a wide distribution of acid strengths, as observed in the NH_3 TPD. Large portions of Al exist outside the framework. The kind of acid sites generated in MCM-22 changed depending on the content of Al. Brønsted acid sites occupy the MCM-22 with $Si/Al_2 = 42$–80. However, Lewis acid sites dominate above this concentration. The MCM-22 is a promising catalyst for shape-selective alkane cracking reactions and Friedel–Crafts acylation.

ACKNOWLEDGMENTS

The authors thank Dr. Hidetaka Kojima and Kazuyuki Matsuoka of Daisel Co., Japan, for the ^{29}Si MAS NMR measurement. We are grateful for the support of the Ministry of Education, Science, Sports and Culture for Grants-in-Aid for Scientific Research in Priority Area 11650809.

REFERENCES

1. Rubin, M. K., and Chu, P., U.S. Patent 4,954,323 (1990).
2. Leonowicz, M. E., Lawton, J. A., Lawton, S. L., and Rubin, M. K., *Science* **264**, 1910 (1994).
3. Asensi, M. A., Corma, A., and Martínez, A., *J. Catal.* **158**, 561 (1996).
4. Corma, A., and Martínez-Triguero, J., *J. Catal.* **165**, 102 (1997).
5. Rodriguez, I., Climent, M. J., Iborra, S., Fornés, V., and Corma, A., *J. Catal.* **192**, 441 (2000).
6. Wu, P., Komatsu, T., and Yashima, T., *Microporous Mesoporous Mater.* **22**, 343 (1998).
7. Niwa, M., and Katada, N., *Catal. Surv. Jpn.* **1**, 215 (1997).
8. Katada, N., Igi, H., Kim, J.-H., and Niwa, M., *J. Phys. Chem. B* **101**, 5659 (1997).
9. Miyamoto, T., Katada, N., Kim, J.-H., and Niwa, M., *J. Phys. Chem. B* **102**, 6738 (1998).
10. Kageyama, Y., Katada, N., and Niwa, M., unpublished data.
11. Miyamoto, Y., Katada, N., and Niwa, M., *Microporous Mesoporous Mater.* **40**, 271 (2000).
12. Katada, N., Kageyama, Y., and Niwa, M., *J. Phys. Chem. B* **104**, 7561 (2000).
13. Katada, N., Miyamoto, T., Begum, H. A., Naito, N., Niwa, M., Matsumoto, A., and Tsutsumi, K., *J. Phys. Chem. B* **104**, 5511 (2000).
14. Corma, A., Corell, C., and Pérez-Pariente, J., *Zeolites* **15**, 2 (1995).
15. Katada, N., Igi, H., Kim, J.-H., and Niwa, M., *J. Phys. Chem. B* **101**, 5969 (1997).
16. Mochida, I., Eguchi, S., Hironaka, M., Nagao, S., Sakanishi, K., and Whitehurst, D. D., *Zeolites* **18**, 142 (1997).
17. Ravishankar, R., Bhattacharya, D., Jacob, N. R., and Sivasanker, S., *Microporous Mater.* **4**, 83 (1995).
18. Kennedy, G. D., Lawton, S. L., and Rubin, M. K., *J. Am. Chem. Soc.* **116**, 11000 (1994).
19. Kolodziejski, W., Zicovich-Wilson, C., Corell, C., Pérez-Pariente, J., and Corma, A., *J. Phys. Chem.* **99**, 7002 (1995).
20. Choudhary, V. R., Sivadinarayana, C., and Kinage, A. K., *J. Catal.* **173**, 243 (1998).
21. Corma, A., Corell, C., Fornés, V., Kolodziejski, W., and Pérez-Pariente, J., *Zeolites* **15**, 576 (1995).
22. Emeis, C. A., *J. Catal.* **141**, 347 (1993).
23. Martens, J. A., Tielen, M., Jacobs, P. A., and Weitkamp, J., *Zeolites* **4**, 98 (1984).
24. Souverijns, W., Verrelst, W., Vanbutsele, G., Martens, J. A., and Jacobs, P. A., *Chem. Commun.* 1671 (1994).
25. Smith, K., Zhenhua, Z., and Hodgson, P. G. K., *J. Mol. Catal. A* **134**, 121 (1998).